J. Synchrotron Rad. (1999). **6**, 381–383

High-quality energy-dispersive XAFS on the 1 s timescale applied to electrochemical and catalyst systems

Andrew Dent,[a*] **John Evans,**[b] **Mark Newton,**[b] **Judith Corker,**[b] **Andrea Russell,**[b] **M B Abdul Rahman,**[b] **Steven Fiddy,**[b] **Rebecca Mathew,**[b] **Richard Farrow,**[a] **Giuseppe Salvini**[a] **and Phillip Atkinson**[a]

[a]Daresbury Laboratory, Daresbury, Warrington, WA4 4AD, UK, [b]Chemistry Dept, University of Southampton, Southampton, SO17 1BJ, UK.
Email: A.J.Dent@dl.ac.uk

A long program involving the development of a fast linear and stable detector, and the recent upgrade of the bent monochromator to a 4-point one at station 9.3 Daresbury Laboratory is showing exciting results such that it has now become possible to obtain analysable XAFS data on 50mM solutions in time scales of a second or less. Three examples of such data are shown: a homogeneous Ni catalyst reaction using a stopped flow system, a heterogeneous catalyst reduction showing time dependent data collected in a microreactor, and an electrochemical system showing the oxidation of small Pt particles as the potential is changed. The improvements have come from two major developments - the monochromator and the detector.

Keywords: EDE, Catalysts, Electrochemistry, Time-resolved, Stopped-Flow

1. Introduction

Energy Dispersive XAFS has been developed at Daresbury on station 9.3 over a number of years and in the last 6 months has culminated in a revolution in the quality of the data which can be collected. Unlike conventional XAFS which relies on a point by point mechanical scanning data collection procedure, dispersive XAFS uses a bent crystal monochromator to disperse a range of X-ray energies. In addition the bending of the monochromator focuses the X-rays onto the sample before then diverging to the detector (Phizackerly R.P. et al., 1983, Dartyge E. et al., 1986, Allinson, N.M. et al., 1988, Hagelstein M, 1989). The detector is a 1024 element photodiode array, which measures the X-ray flux at each pixel and can be readout in less than 1ms. Depending on the sample it takes 2-30ms to saturate the detector, thus it is possible to collect a full XAFS spectrum in this time. Typically though 50-500 scans are collected to improve the signal to noise, but this still means high quality data can be collected in under one second.

2. Monochromator

Traditionally these types of horizontally diffracting monochromators, which are in widespread use throughout synchrotrons, use a triangular crystal. This is because simple engineering geometry indicates that clamping the triangle at the base and pushing at the tip forms it into a cylinder. However it can be shown that the focal spot is not uniform but has a cusp form due to errors such as imperfect clamping, heating effects, not being able to push at the point, and the fact that the ideal surface is actually an ellipse. This works acceptably for many situations, and sophisticated designs which shape the triangle to obtain better focal spots and allow it to be cooled have been developed (Allen P.G. et al. 1993, Bliss N. et al., 1995). The 4-point bender gets around these problems by using a rectangular crystal to which a separate couple can be applied at each end. It is effectively a mirror bender mechanism on its side, (see figure 1) and in principle it is similar to those of Hagelstein M. et al. 1996, Allen P.G. et al. 1993, Lee P.L. et al. 1994 and Brauer S. et al. 1996, but was designed and built using a simple lever and cam mechanism to apply the couples. Tests have shown that by applying an uneven couple to each end of the crystal, an elliptical bend can be obtained. This leads to a uniform focal spot, which moreover is much smaller (90μm FWHM) and will therefore pass through a 200μm slit. The theoretical minimum FWHM is 40μm that hopefully will be achieved in the future when additional profiling is done (Pellicer-Porres J. et al. 1998). The later is important for high pressure XAFS the diamond anvil cells used to pressurise the material typically have sample sizes of 100-300μm.

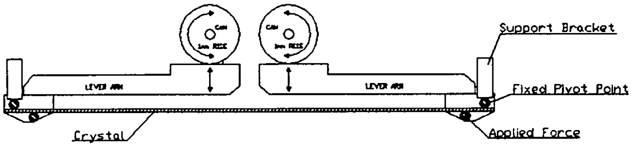

Figure 1 Plan view of crystal bender showing the lever arms and cams that are used to apply a bending couple to the crystal.

3. Detector

Considerable effort has been put into testing and evaluating commercially available photodiode arrays by the Daresbury detector group (Bogg D. et al., 1997). The final choice was a Hamamatsu S4874 which gave the lowest noise and, most critically, the smallest non-linearity of better than 0.2%. Given that the XAFS oscillations above an absorption edge are at best a few %, and beyond the edge much less than this, any non-linearity quickly become apparent as non-statistical noise. The detector is also radiation hard and has suffered minimal radiation damage despite being in the direct beam from a Wiggler station. Precision clock driving electronics and a low noise preamplifier have been designed. These have been carefully integrated into a VME data acquisition system which allows real time data collection and control of experimental equipment such as a stopped-flow device or electrochemical potentiostat which might be used to trigger chemical changes in the sample.

4. Ni Homogeneous Catalysis

A good example of the speed and quality of data that can now be achieved is shown in stopped flow reactions of homogeneous

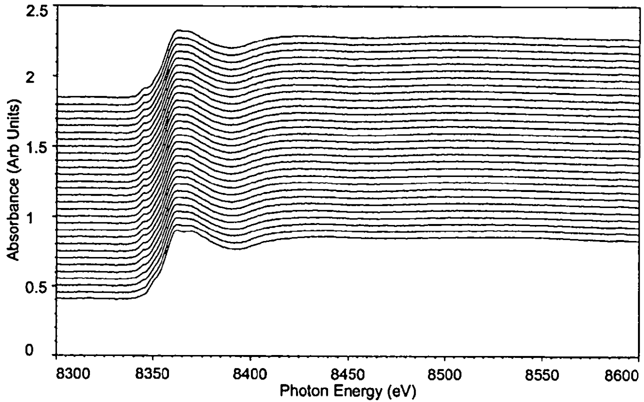

Figure 2 Reaction of $Ni(dpm)_2$ with $AlEt_2(OEt)$. Stack plot of 30 frames, each of 2 s acquisition time. (Time = 0 s bottom, time = 60 s top.)

catalysts. Previous work has shown activation of nickel complexes for alkene oligomerisation catalysis can be followed by XAFS (Bogg D. et al., 1996). In the reaction of $[Ni(dpm)_2]$ ($dpm{=}Bu^tC(O)CHC(O)Bu^t$) with $AlEt_2OEt$ which forms organometallic complexes one syringe contains the nickel bis diketonate complex in hex-1-ene and toluene, and the second syringe contains the diethyl aluminium diethyloxide. Figure 2 shows a plot of the time resolved data which is about 60mM Ni concentration. Each spectrum consists of 100 accumulations of 20ms each, ie. 2 seconds data collection. The growth of the pre-edge feature and change at the top of the edge can be clearly seen. Figure 3 shows an analysis of the final spectrum. We know from previous static work (Bogg D. et al., 1996) that the likely structure is 2 O at 1.92Å from the diketonate ligand and 2-3 C at 2.03Å from the alkyl ligands. Within the quality of this data only 1 shell of 3–4 carbons/oxygens at 1.90Å could be fitted, but this shows that some analysis can be carried out on data collected in such a short time.

5. Pt Heterogeneous Catalysis

Platinum-tin and platinum catalysts are also widely used in the petrochemical industry for example in reforming or in isobutane dehydrogenation. Work has been done on Pt-Sn catalysts but little has been done on Pt-Ge systems, but these have also been shown to have many good properties and may also (similar to Pt-Sn) increase the lifetime of these catalysts due to reduced activity via coking. As an example of some of the data obtained 5% $Pt(acac)_2$ on SiO_2, was reduced under 10% H_2 in N_2 flowing at approximately 8ml/min (acac=MeC(O)CHC(O)Me). Figure 4 shows the raw XAFS data plotted about every minute as the temperature was ramped at 4.2°C/min. Each spectrum is 100 scans of 120ms (12s data collection time). Figure 5 shows the Fourier transformed data and the reduction from an oxide environment to Pt metal particles can be clearly seen. Not shown here due to lack of space is similar data collected on both Pt and Ge edges simultaneously and at 1% Pt concentrations. Thus the technique has potential to understand how changing the Ge additives affects the size of the Pt particles and their subsequent stability to de-activation by sulfurisation.

6. Pt Electrochemical Oxidation

The following example shows how dispersive XAFS allows the electrochemical oxidation of small Pt particles to be monitored in real time as the potential is scanned. The cell is bases on a design by Herron M.E. et al. (1992) and has 3 electrodes: working

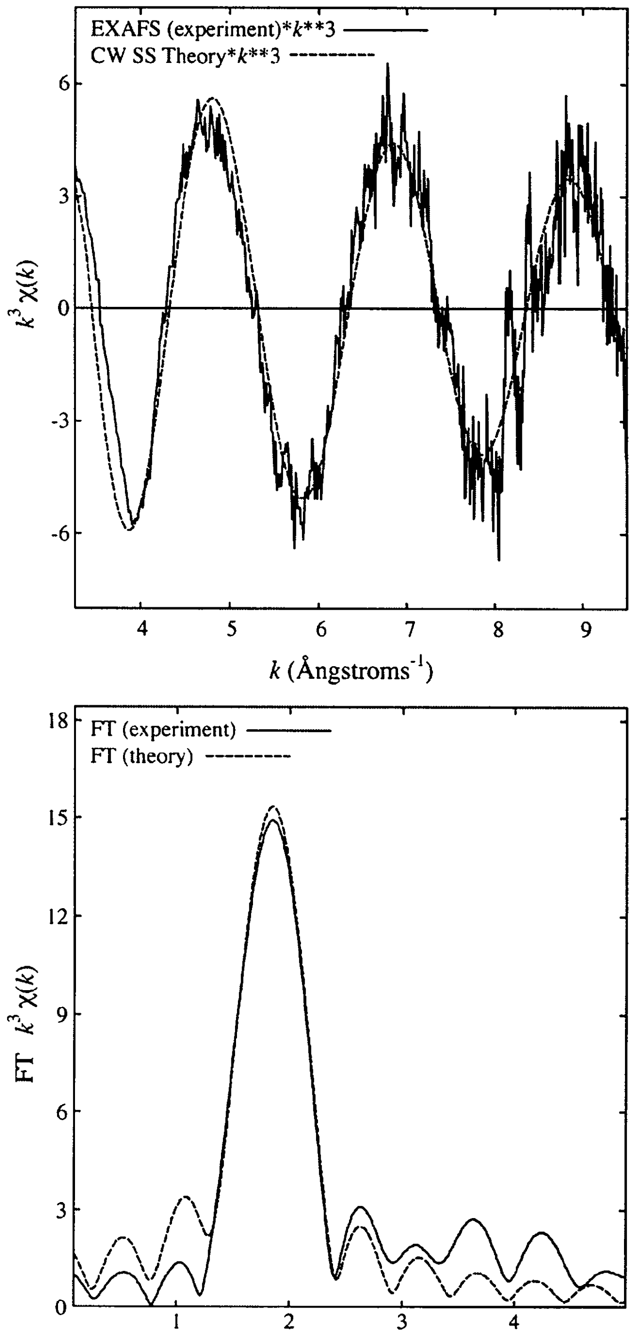

Figure 3 k^3 weighted χ spectrum and Fourier transform modulus for the final spectrum (ie top) of figure 2. The model fit is shown as a broken line.

electrode, Pt gauze counter electrode and mercury/mercurous sulphate (mms) reference electrode. The working electrode consists of 40 wt% Pt on XC-72R carbon from Johnson Matthey mixed with 15% Nafion® binder and then deposited on TGPH-120 carbon paper from E-Tek. It is known that at –600mV H atoms adsorb/desorb from the surface (not seen with XAFS!) so only Pt–Pt interactions are seen with usually 8–10 neighbours. As the potential is swept through 0V, no changes are seen until about +200mV an oxide begins to form on the Pt. The number of Pt neighbours falls to about 7–9 and 1–2 oxygen neighbours can be seen. Figure 6 shows the XAFS data collected every 20s as the potential was swept at 5.5mV/s, thus the spectra are shown at

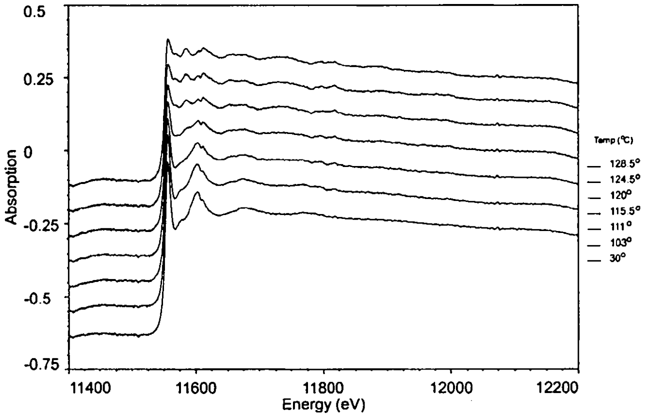

Figure 4 Pt XAFS spectra showing the reduction of 5% Pt(acac)$_2$ on SiO$_2$ to Pt particles. 12s data collection time, spectrum taken every minute. The distortions close to 11800 and 12100 are due to crystal glitches not normalising completely.

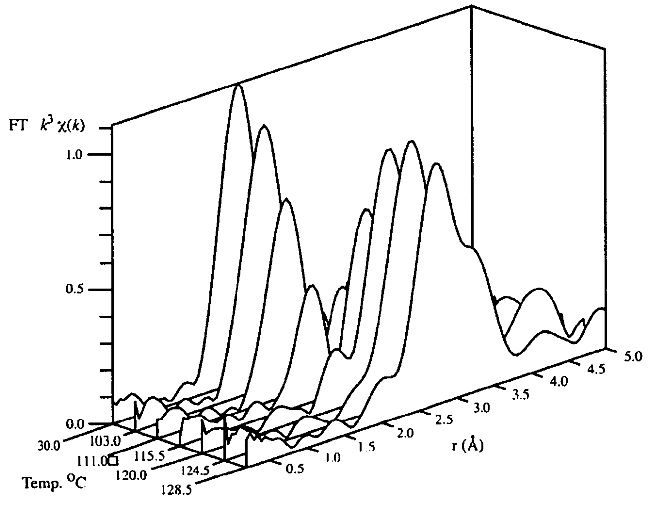

Figure 5 Fourier transform modulli of data from figure 4 showing the progression of the Pt environment from predominately Pt–O bonds to Pt–Pt.

approximate 100mV intervals. Each spectrum was the sum of 300 readouts of 17ms integration time (5 s total data collection time). The white line is seen to increase steadily after +200mV thus showing the oxidation of the Pt.

7. Conclusion

In conclusion these developments and experiments show that it is possible in these samples to see XANES and pre-edge changes in 20–30ms and subtle XANES changes in 100–200ms. We have established that analysable XAFS data can be collected in 1–2s and high quality data comparable with that collected in normal scanning mode be collected in 10–20s.

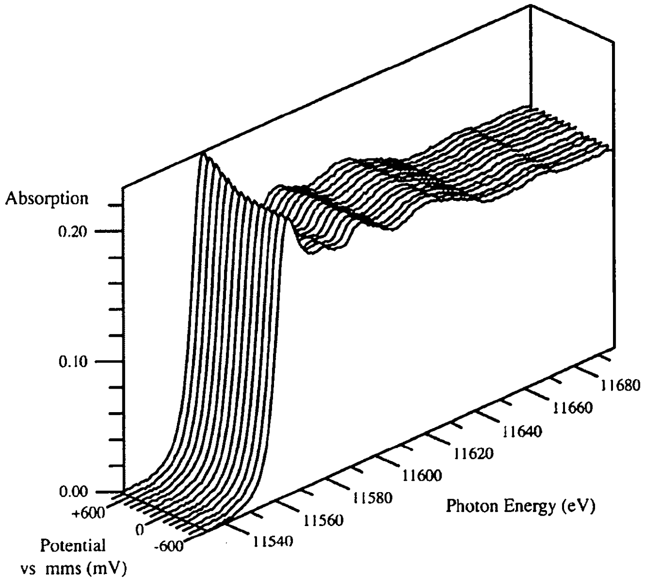

Figure 6 Pt XAFS spectra collected as potential in electrochemical cell varied from –600 to +600mV. 5s data collection per spectrum.

8. References

Allen P.G., Conradson S.D. and Penner-Hahn, J.E., (1993) J. Appl. Cryst., 26(3), 172-179.

Allinson N.M., Baker G., Greaves G.N. and Nicoll J.K., (1988) Nucl. Inst. Meth. A266, 592-597.

Bliss N., Bordas J., Fell B.D., Harris N.W., Helsby W.I., Mant G.R., Smith W. and Towns-Andrews E., (1995) Rev. Sci. Instrum., 66(2), 1311-1313.

Bogg D., Conyngham M., Corker J.M., Dent A.J., Evans J., Farrow R.C., Kambhampati V.L., Masters A.F., Mcleod D.N., Ramsdale C.A. and Salvini G., (1996) Chem. Commun., 647-648.

Bogg D., Dent A.J., Derbyshire G.E., Farrow R.C., Ramsdale C.A. and Salvini G., (1997) Nucl. Instrum. Meth., A392, 461-464.

Brauer S., Rodricks B., Assoufid L., Beno M. and Knapp G., (1996) Rev. Sci. Instrum. 67, 3349.

Dartyge E., Depautex C., Dubuisson J.M., Fontaine A., Jucha A., Leboucher P. and Tourillon G., (1986) Nucl. Inst. Meth. A246, 452.

Hagelstein M., Cunis S., Frahm R., Niemann W. and Rabe P., (1989) Physica B, 158, 324.

Hagelstein M., San Miguel A., Fontaine A. and Goulon J., (1996) C2, J. Phys. IV, (Suppl. J. de Phys. III), C2-303—308.

Herron M.E., Doyle S.E., Pizzini S., Roberts K.J., Robinson J., Hard G. and Walsh F.C., (1992) J. Electroanal. Chem., 324, 243.

Lee P., Beno M.A., Jennings G.,Ramanathan, M., Knapp G.S., Huang K., Bai J. and Montano P.A., (1994) Rev. Sci. Instrum. 65, 1.

Pellicer-Porres J., San Miguel, A. and Fontaine A., (1998) J. Syn. Rad. 5, 1250.

Phizackerley R.P., Rek Z.V., Stephenson G.V., Conradson S.D., Hodgson K.O., Matsushita T. and Oyanagi Y., (1983) J. Appl. Phys. 16, 220.

(*Received 10 August 1998; accepted 29 January 1999*)